Rationale of 5-^{125}I-Iodo-4′-Thio-2′-Deoxyuridine as a Potential Iodinated Proliferation Marker

Jun Toyohara, MS[1]; Akio Hayashi, PhD[1]; Mikiko Sato, MS[1]; Hiromichi Tanaka, PhD[2]; Kazuhiro Haraguchi, PhD[2]; Yuichi Yoshimura, PhD[2]; Yoshiharu Yonekura, MD, PhD[3]; and Yasuhisa Fujibayashi, PhD, DMedSci[3]

[1]*Research and Development Division, Research Center, Nihon Medi-Physics Company, Limited, Chiba, Japan;* [2]*School of Pharmaceutical Science, Showa University, Tokyo, Japan; and* [3]*Biomedical Imaging Research Center, Fukui Medical University, Fukui, Japan*

The aim of this investigation was to synthesize and test a novel metabolically stable iodinated nucleoside as a proliferation-imaging agent for SPECT. **Methods:** 5-Iodo-4′-thio-2′-deoxyuridine (ITdU) and 5-iodo-1-(4-thio-β-D-arabinofuranosyl)uracil (ITAU) were tested. The radiolabeling of ITdU and ITAU with ^{125}I was achieved by a destannylation reaction of the trimethylstannyl precursor of each nucleoside. The products were isolated in high yields and with >99% radiochemical purities. **Results:** ^{125}I-ITdU was effectively phosphorylated by cytosolic nucleoside kinases and specifically incorporated into a thymidine kinase–expressing L-M cell rather than a thymidine kinase–deficient mutant L-M (TK$^-$) cell. In addition, an in vitro cell metabolism study of ^{125}I-ITdU clarified that ^{125}I-ITdU was effectively and specifically incorporated into a DNA fraction (>90% at 60 min). Therefore, ^{125}I-ITdU was proven to be an ideal DNA synthesis marker such as 5-^{125}I-iodo-2′-deoxyuridine (IUdR). In contrast, ^{125}I-ITAU was neither remarkably phosphorylated by cytosolic nucleoside kinases nor notably incorporated into an L-M cell rather than an L-M (TK$^-$) cell. ^{125}I-ITdU and ^{125}I-ITAU showed a higher resistance to phosphorolytic cleavage by recombinant thymidine phosphorylase than did ^{125}I-IUdR. Furthermore, biodistribution of ^{125}I-ITdU and ^{125}I-ITAU revealed better in vivo stability of radioiodination than that of ^{125}I-IUdR. ^{125}I-ITdU also displayed a significantly higher uptake in proliferating organs (thymus, spleen, small intestine, and bone) than in nonproliferating organs (brain, muscle, liver, and lung), as did ^{125}I-IUdR, at 18 h after injection. As indicated by the in vitro study, ^{125}I-ITAU did not show any significant uptake in proliferating organs. **Conclusion:** Radioiodine-labeled ITdU is potentially useful as a proliferation-imaging agent, and further studies should clarify the usefulness of this compound as a tumor-imaging agent.

Key Words: 5-^{125}I-iodo-4′-thio-2′-deoxyuridine; 5-^{125}I-iodo-1-(4-thio-β-D-arabinofuranosyl)uracil; 5-^{125}I-iodo-2′-deoxyuridine; nucleoside kinases; thymidine phosphorylase

J Nucl Med 2002; 43:1218–1226

Halogenated thymidine analogs such as 5-iodo-2′-deoxyuridine (IUdR) can be successfully used as cell proliferation markers for in vitro studies because these compounds are rapidly incorporated into newly synthesized DNA. Therefore, IUdR has been evaluated as a potential in vivo tracer in nuclear medicine (*1–2*); however, the image quality and the calculation of proliferation rates are impaired by its rapid in vivo degradation. The C–N glycosidic bond of IUdR is too labile in vivo, and that feature leads to metabolites with reduced tumor affinity.

It is well known that the 3′- or 2′-substitution of a sugar moiety with electronegative fluorine will stabilize the N-glycosidic bond of nucleosides. Recently, the 3′-fluorinated 2′-deoxy-5-iodouridine analog (DFIU) has been designed and tested (*3*). The strategy of stabilizing the C–N glycosidic bond by introducing the fluorine substitution was successful, but ^{123}I-DFIU did not show improved tumor-to-background ratios because of its high background activity. Therefore, DFIU is not a promising tumor-imaging agent. There is evidence that the 3′-substitution with electronnegative fluorine lowers the nucleoside transport activity of the cell membrane and the affinity to thymidine kinase (*4,5*). The introduction of fluorine to the 2′-position of IUdR, 5-iodo-1-(2-fluoro-2-deoxy-β-D-ribofuranosyl)uracil (FIRU), also resulted in resistance to N-glycoside deglycosylation and dehalogenation. However, this modification deteriorated cytosolic thymidine kinase phosphorylation (*6*). The absence of tumor-selective uptake that was observed with ^{131}I-FIRU makes it unsuitable as an imaging agent. The introduction of fluorine to the 2′-up position of IUdR, 5-iodo-1-(2-fluoro-2-deoxy-β-D-arabinofuranosyl)-uracil (FIAU), was also resistant to deglycosylation and showed a significant uptake in the herpes simplex virus thymidine kinase transfected tumor. However, FIAU showed only a background level of uptake in the host mammalian thymidine kinase that expresses MCA26 tumor (*7*). The 2′-up stereochemistry exhibited in FIAU was more efficiently phosphorylated by the mitochondrial thymidine kinase (TK_2) and resulted in the incorporation of mitochondrial DNA (*8*). TK_2 is expressed at low but constant levels

Received Nov. 25, 2001; revision accepted May 6, 2002.

For correspondence or reprints contact: Yasuhisa Fujibayashi, PhD, DMedSci, Biomedical Imaging Research Center, Fukui Medical University, 23 Shimoaizuki, Matsuoka-cho, Yoshida-gun, Fukui, 910-1193, Japan.
E-mail: yfuji@fmsrsa.fukui-med.ac.jp

in all cells and has no correlation with the cell cycle. We have shown that TK_2-specific substrate arabinothymidine uptake did not correlate with tumor cell proliferation (*9*). Therefore, a TK_2-selective substrate such as FIAU is not considered to be an identical proliferation-imaging agent.

On the basis of the above considerations, we concluded that there are inherent limitations in drug design using 2′- and 3′-substitution with electronegative residues. Therefore, we need a new strategy for stabilizing the C–N glycosidic bond without interfering with the cytosolic thymidine kinase. The resistance of several 4′-thio-ribonucleosides to bacterial cleavage and of 4′-thioinosine to cleavage by purine nucleoside phosphorylase has been reported (*10,11*). These results suggested that the replacement of the furanose ring oxygen with sulfur might also generally confer resistance to phosphorylase. Therefore, it is logical to assume that 4′-thio derivatives of 5-iodo-2′-deoxyuridine would also be resistant to phosphorolytic cleavage and could be phosphorylated by a thymidine kinase without largely changing the stereochemistry of 5-iodo-2′-deoxyuridine. In our study, we synthesized and tested 5-^{125}I-iodo-4′-thio-2′-deoxyuridine (ITdU). We also synthesized and tested 5-^{125}I-iodo-1-(4-thio-β-D-arabinofuranosyl)uracil (ITAU).

MATERIALS AND METHODS

Radiochemicals

Carrier-free sodium ^{125}I-iodide and 5-^{125}I-iodo-2′-deoxyuridine (74 TBq/mmol) were purchased from Amersham Pharmacia Biotech (Buckinghamshire, U.K.). The specific activity of 5-^{125}I-iodo-2′-deoxyuridine was adjusted to 37 MBq/μmol with unlabeled 5-iodo-2′-deoxyuridine purchased from Aldrich (Milwaukee, WI).

Synthesis of 5-Trimethyltin-4′-Thio-2′-Deoxyuridine

ITdU (Figs. 1 and 2A) was synthesized as reported (*12*). ITdU (9.5 mg, 0.026 mmol), bis(trimethyltin) (17.3 mg, 0.052 mmol), and bis(triphenylphosphine)palladium(II)dichloride (5 mg) were dissolved in 1,4-dioxane (3 mL), and the mixture was refluxed for 3 h under an argon atmosphere. The solvent was removed by rotary evaporation, and the desired product, 5-trimethyltin-4′-thio-2′-deoxyuridine ($(CH_3)_3$Sn-TdU) (6.9 mg, 65%), was purified by preparative silica gel thin-layer chromatography (TLC) (chloroform/methanol, 6:1).

^{1}H NMR (270 MHz, CD_3OD) δ 0.26 (s, 9H, $(CH_3)_3$Sn), 2.26 (ddd, 1H, J = 4.6, 7.9, 13.2 Hz, 1H, H-2′), 2.27 (ddd, J = 4.6, 6.6, 13.4 Hz, 1H, H-2′), 3.41 (m, 1H, H-4′), 3.71 (dd, J = 5.9, 11.2 Hz, 1H, H-5′), 3.80 (dd, J = 4.6, 11.2 Hz, 1H, H-5′), 4.47 (m, 1H, H-3′), 6.41 (dd, J = 7.9, 6.6 Hz, 1H, H-1′), 7.93 (s, 1H, H-5).

Synthesis of 5-Trimethyltin-1-(4-Thio-β-D-Arabinofuranosyl)Uracil

ITAU (Figs. 1 and 2B) was synthesized as reported (*13*). ITAU (4.0 mg, 0.010 mmol), bis(trimethyltin) (6.6 mg, 0.020 mmol), and bis(triphenylphosphine)palladium(II)dichloride (5 mg) were dissolved in 1,4-dioxane (5 mL), and the mixture was refluxed for 4 h under an argon atmosphere. The solvent was removed by rotary evaporation, and the desired product, 5-trimethyltin-1-(4-thio-β-D-arabinofuranosyl)uracil ($(CH_3)_3$Sn-TAU) (2.3 mg, 55%), was purified by preparative silica gel TLC (chloroform/methanol, 3:1).

^{1}H NMR (270 MHz, CD_3OD) δ 0.7 (s, 9H), 3.55–3.67 (m, 1H), 3.77–3.95 (m, 2H), 4.07 (t, J = 5.9 Hz, 1H), 4.16 (t, J = 5.9, 1H), 6.28 (d, J = 5.3 Hz, 1H), 8.03 (s, 1H).

Synthesis of ^{125}I-ITdU

Fifty microliters of ^{125}I-NaI (33 MBq in 0.1N NaOH) and 4.7 μL iodine (60 μg, 0.47 μmol in chloroform) were added to a reaction vial containing 1 mL water and 1 mL chloroform. The vial was spun in a vortex for 10 s, and the aqueous phase was removed. Then, 100 μL $(CH_3)_3$Sn-TdU (Figs. 1 and 2A) solution (100 μg, 0.25 μmol in ethyl acetate) was added to the vial, and it was allowed to stand for 2 h at room temperature. The labeling reaction was terminated by the addition of 1 drop of 1N sodium metabisulfite, and the chloroform was evaporated by heating the mixture at 60°C. The labeled compound was purified using a Sep-Pak QMA cartridge (Waters, Milford, MA), and the labeling yield was 22% (7.3 MBq) with a radiochemical purity of approximately 100%. The specific activity of ^{125}I-ITdU (Figs. 1 and 3A) was calculated to be approximately 29.2 MBq/μmol.

Synthesis of ^{125}I-ITAU

Fifty microliters of ^{125}I-NaI (67 MBq in 0.1N NaOH) and 4.7 μL iodine (60 μg, 0.47 μmol in chloroform) were added to a reaction vial containing 1 mL water and 1 mL chloroform. The vial was spun in a vortex for 10 s, and the aqueous phase was removed. Then, 100 μL $(CH_3)_3$Sn-ITAU (Figs. 1 and 2B) solution (100 μg, 0.24 μmol in ethyl acetate) was added to the vial, and it was allowed to stand for 2 h at room temperature. The labeling reaction was terminated by the addition of 1 drop of 1N sodium metabisulfite, and the chloroform was evaporated by heating the mixture at 60°C. The labeled compound was purified using a Sep-Pak QMA cartridge, and the labeling yield was 26% (17.3 MBq) with a radiochemical purity of approximately 100%. The specific activity of ^{125}I-ITAU (Figs. 1 and 3B) was approximately 72.1 MBq/μmol.

Nucleoside Kinase Assay

Nucleoside kinase activity was assayed on the basis of the precipitation of nucleoside monophosphates with lanthanum chloride (*14*). Cytosolic nucleoside kinases were prepared from the

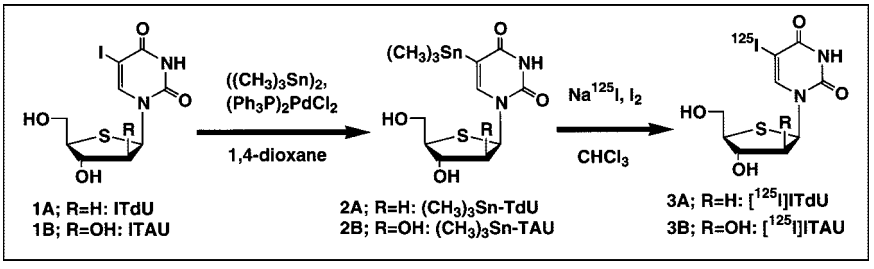

FIGURE 1. Synthetic pathway for preparation of radiolabeled ITdU and ITAU by destannylation.

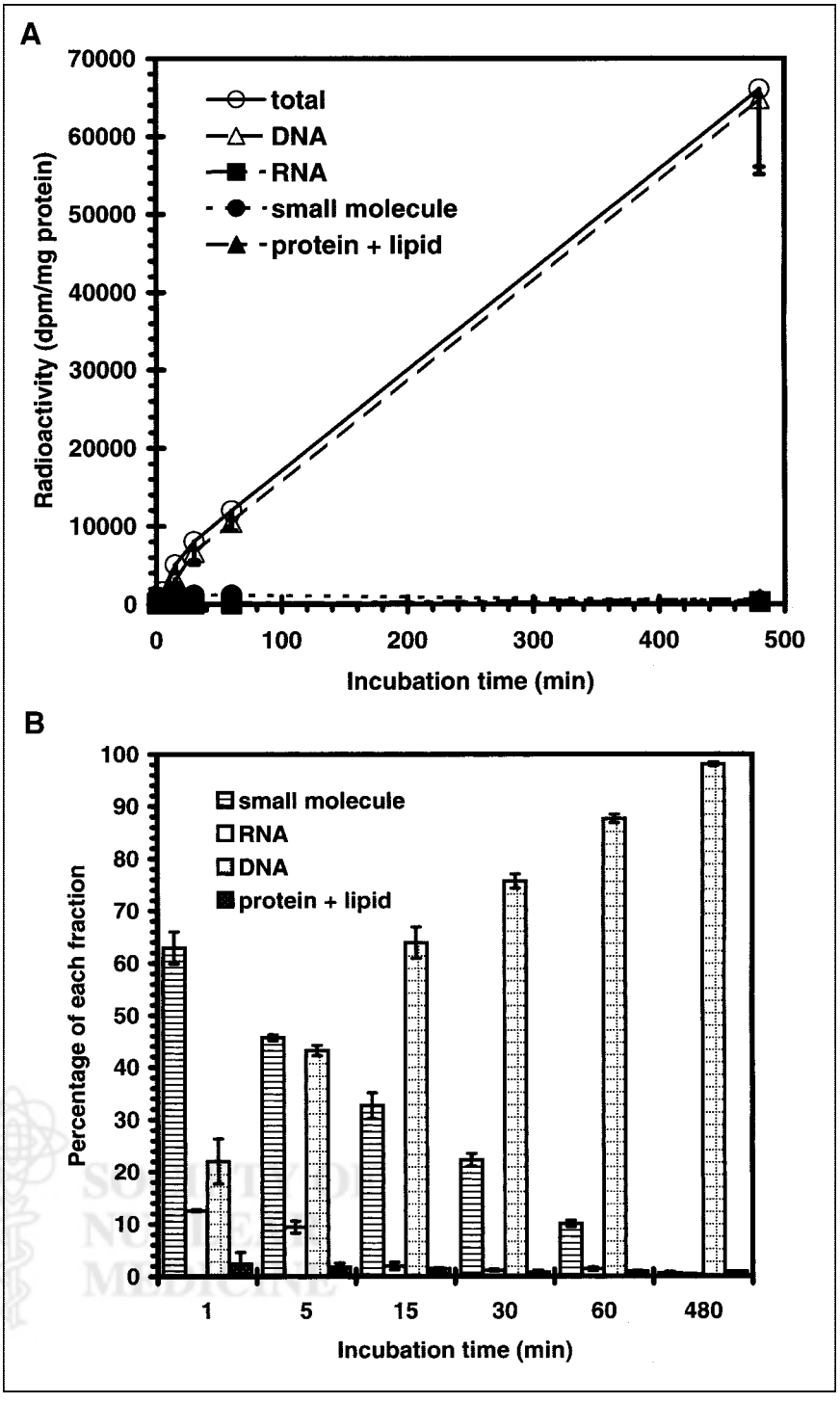

FIGURE 2. Time-dependent incorporation of radioactivity into Lewis lung carcinoma cells. (A) Radioactivity of acid-soluble small molecule, DNA, RNA, and protein fractions is shown. (B) Time-dependent percentage of radioactivity distribution in each fraction of Lewis lung carcinoma. Data are expressed as mean ± SD for 3 experiments.

Lewis lung carcinoma (LL/2), purchased from Dai-Nippon Seiyaku Co., Ltd. (Osaka, Japan) and maintained in their recommended culture media, which were obtained from the manufacturer. The cell lines were grown in a 5% CO_2-humidified atmosphere at 37°C. Exponentially growing tumor cells in a 100-mm plate were washed 3 times with ice-cold phosphate-buffered saline (PBS) and scraped into the 1.5-mL tube. After centrifugation, the resultant cell pellet was suspended in 0.5 mL of homogenized buffer (10 mmol/L Tris-HCl [pH 7.5], 1 mmol/L ethylenediaminetetraacetic acid [pH 8.0], 5 mmol/L 2-mercaptoethanol) and homogenized by freeze-thawing. The homogenates were then centrifuged at 105,000*g* at 4°C for 60 min. The total protein concentration of cytosol was determined with a Bio-Rad protein assay kit (Bio-Rad, Richmond, CA), using bovine serum albumin as the standard. The reaction mixture for the assay of nucleoside kinases contains, per 0.1 mL, 50 mmol/L Tris-HCl buffer (pH 7.5), 2.5 mmol/L adenosine triphosphate, 2.5 mmol/L $MgCl_2$, 2 nmol nucleoside (approximately 0.074 MBq), and 0.1

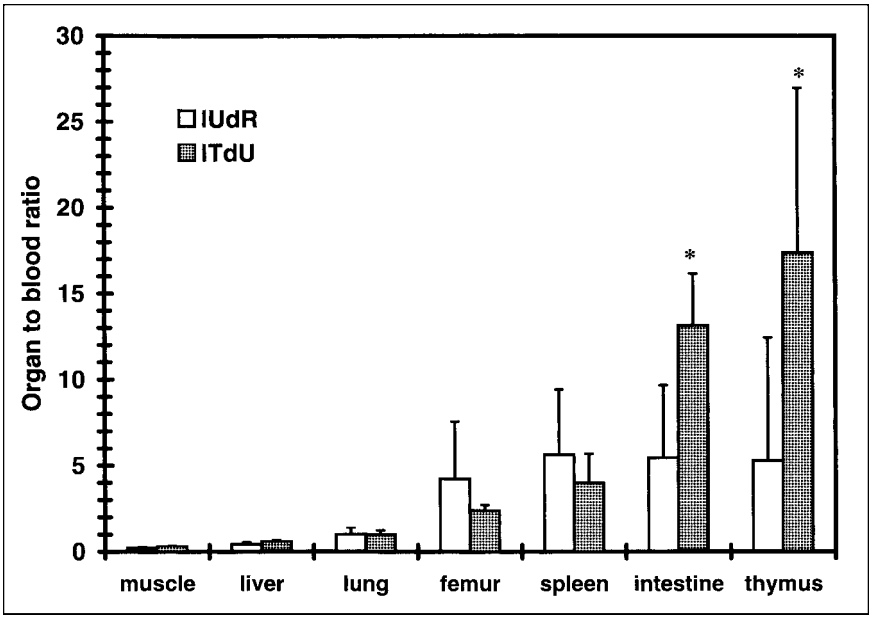

FIGURE 3. Uptake of iodonucleosides, expressed as organ-to-blood ratio of radioactivity. Animals were killed at 18 h after injection. Data are expressed as mean ± SD for 3 experiments. Iodonucleosides showed higher uptake in proliferation organs (femur, spleen, intestine, and thymus) than in nonproliferating organs (muscle, liver, and lung). Statistical significance between ^{125}I-IUdR uptake and ^{125}I-ITdU uptake was observed in intestine and thymus ($P < 0.05$; Student t test).

mg cytosol. The reaction was performed at 37°C for 60 min and then terminated by adding 1 mL $LaCl_3$ solution (100 mmol/L $LaCl_3$ and 5 mmol/L triethanolamine) to precipitate all of the phosphorylated compounds in the mixture. Background samples were assayed in the same manner except that the homogenized buffer was used in place of cell cytosol. The samples were spun vigorously in a vortex, and the precipitate was collected. The pellets were washed once with 1 mL $LaCl_3$ solution, and the radioactivity associated with the precipitate was determined by an auto well gamma counter (ARC-380; ALOKA, Tokyo, Japan). The specific radioactivity was calculated by subtracting the background counts from the sample counts. The enzyme activity was expressed as picomoles of phosphorylated compound per milligram of protein per hour.

Recombinant Thymidine Phosphorylase Assay

To evaluate the stability of the C–N glycosidic bond, we tested the recombinant thymidine phosphorylase cleavage reaction. The reaction mixture for the assay of recombinant thymidine phosphorylase contains, per 0.125 mL, 168 mmol/L potassium phosphate buffer (pH 7.6), 2 nmol nucleoside (0.074 MBq), and several units (0.9 milliunits to 9 units) of recombinant thymidine phosphorylase (Sigma Chemical Co., St. Louis, MO). The reaction was performed at 25°C for 30 min and then terminated by heating at 100°C for 3 min. After the precipitate was removed, a 1-μL aliquot of the reaction mixture was applied to a silica gel plate (Sil60 F254; Merck, Schuchardt, Germany) with standards for nucleoside. Then, the resultant metabolite 5-iodouracil (IU) was separated by TLC using the solvent system consisting of chloroform/isopropyl alcohol (3:1). The spot of IU was identified under an ultraviolet (UV) ray by comparison with the standards. The radioactivity in the UV spot of IU was scraped and measured by an auto well gamma counter (ARC-380). In some experiments, the radioactivity on the plate was measured by a bioimaging analyzer (BAS-1500; Fuji Photo Film Co., Tokyo, Japan). Data were expressed as picomoles of formed IU per unit/30 min.

Cell Uptake Study with LL/2, L-M, and L-M (TK⁻) Cell Lines

LL/2, L-M, and L-M (TK⁻) cell lines were purchased from Dai-Nippon Seiyaku Co., Ltd., and were maintained in the recommended culture media, which were obtained from the manufacturer. The cell lines were grown in a 5% CO_2-humidified atmosphere at 37°C. The L-M (TK⁻) cell line lacks thymidine kinase activity. To clarify the thymidine kinase–specific incorporation of the nucleoside, we compared the cell uptake of nucleosides between the L-M parent cell and its TK mutant cell line L-M (TK⁻). The cells were harvested and seeded at a concentration of 2.0×10^5 into 24-well plates, and the tracer uptake experiment was performed 24 h after seeding. Dulbecco's modified Eagle medium (GIBCO, Grand Island, NY) supplemented with 10% calf serum (GIBCO) was used as the assay medium. On the basis of the thymidine concentration of the calf serum, the thymidine concentration of the assay medium was estimated to be 11.7 μg/L (48.3 nmol/L), which is close to the physiologic thymidine concentration in human serum (*15*). Briefly, 500 μL of assay medium containing 2 nmol (0.074 MBq) of each tracer was added to each well, and the plate was incubated at 37°C for 60 min. After incubation, the medium was removed, and the cells were washed 3 times with ice-cold PBS. After the washing, cell lysis was performed with 500 μL of 0.2N NaOH, and the radioactivity in the lysate was counted with an auto well gamma counter (ARC-380). The protein content of the lysate was then measured with Bio-Rad Detergent-Compatible protein assay reagent (Bio-Rad). The radioactivity remaining in the well of the plate after lysis of the cells was <5% of the total radioactivity. Cell cycle measurements were also performed under the same experimental conditions. The cell lines were harvested and seeded at a concentration of 2.0×10^5 into 24-well plates. After 24 h of incubation, cells from 5 wells were exposed to trypsin and collected in a 15-mL culture tube (Falcon; Becton Dickinson, Lincoln Park, NJ). The cells were sedimented by centrifugation and treated with CycleTEST PLUS DNA Reagent Kit (Becton Dickinson, San Jose, CA) to prepare samples for DNA analysis on a flow cytometer according to the manufacturer's

instructions. The cell cycle profiles of the samples were analyzed by flow cytometry (FACS Caliber; Becton Dickinson, Franklin Lakes, NJ), and the percentage of the S-phase cell fraction was calculated by Mod-Fit LT software (Becton Dickinson, San Jose, CA).

DNA Incorporation

DNA extraction using a quantitative acid extraction technique was performed on separate small molecules, RNA, DNA, and macromolecules (*16*). Cultured LL/2 cell lines were harvested and seeded at a concentration of 58×10^5 into a 100-mm dish (Falcon; Becton Dickinson, Lincoln Park, NJ), and the DNA extraction was performed 24 h after seeding. Briefly, 5 mL of assay medium containing 1.11 MBq of tracer was added to each dish, and the dish was incubated at 37°C for various lengths of time. After incubation, the medium was removed, and the cells were washed 2 times with ice-cold PBS. After the washing, the cells were harvested by scraping and collected by centrifugation. The cells were then homogenized in 1 mL of ice-cold 0.2N $HClO_4$ by freeze-thawing. After cooling on ice for 10 min, the homogenates were centrifuged at 1,200*g* at 4°C for 10 min. The acid-soluble fraction was removed, and the radioactivity was determined by an auto well gamma counter (ARC-380). The acid-insoluble precipitate was resuspended in 2 mL of 0.66 mg/mL type III ribonuclease (Sigma Chemical Co.; 68 Kunitz U/mg) in 0.1 mol/L *N*-(2-hydroxyethyl)piperazine-*N*′-(2-ethanesulfonic acid) (pH 7.6) and incubated at 37°C for 30 min, after which 0.5 mL of ice-cold 5N $HClO_4$ was added. After cooling and centrifugation, the supernatant fluid containing RNA was removed, and the radioactivity was determined. The remaining precipitate was resuspended in 1 mL of 1N $HClO_4$ and incubated at 90°C for 15 min. After cooling and centrifugation, the supernatant containing DNA hydrolysates was removed, and the radioactivity was determined. The pellet was washed once with 1 mL of ice-cold 1N $HClO_4$. The remaining proteins and lipids were solubilized by 1N NaOH, and the radioactivity was determined.

Biodistribution in Normal Mice

Nine-week-old C57BL/6 mice were purchased from Japan SLC, Inc. (Shizuoka, Japan) and were held for 1 wk before the study. All procedures were performed in accordance with the institutional guidelines (Guidelines for Animal Experiments, Fukui Medical University). A saline solution of 0.05 mL containing 5 nmol ^{125}I-labeled nucleoside (0.19 MBq) was administered as a bolus through the tail vein. The mice were killed by blood removal from the heart under ether anesthesia at predesigned time intervals of 1, 1.5, 2, 8, and 18 h. Three animals were killed at each time point. Urine was collected throughout the experiment, and blood samples were obtained from the syringe that was used in killing the animals. The main organs were removed and weighted and, together with the blood, urine samples were counted in an auto well gamma counter (ARC-380). The percentage dose per organ and the percentage dose per gram of tissue were calculated without body weight normalization.

TABLE 1
Relative Phosphorylation of Iodonucleosides by Nucleoside Kinases

Nucleoside	pmol phosphorylated*	Relative potency
IUdR	1,620.8 ± 123.4	1.00
ITdU	802.4 ± 67.9	0.50
ITAU	13.3 ± 0.6	<0.01

*pmol phosphorylated = pmol/mg protein/h.

TABLE 2
Susceptibility of Iodonucleosides to Glycosidic Bond Cleavage

Nucleoside	pmol IU formed*	Relative IU formation
IUdR	138,606.2 ± 14,902.3	1.00
ITdU	3,778.7 ± 692.0	0.03
ITAU	514.8 ± 367.0	<0.01

*pmol IU formed = pmol/unit/30 min.

RESULTS

Relative Phosphorylation of Iodonucleosides by Nucleoside Kinases

Table 1 shows the results of the phosphorylation of iodonucleosides by nucleoside kinases. The relative phosphorylation potency, which is normalized to IUdR as 1.0, is also indicated. ^{125}I-ITdU was phosphorylated by nucleoside kinases and shows half of the activity of IUdR. ^{125}I-ITAU was slightly phosphorylated, although the relative phosphorylation potency was <0.01.

Susceptibility of Iodonucleosides to Glycosidic Bond Cleavage

Table 2 shows the results of the recombinant thymidine phosphorylase assay. The relative IU formations, which were normalized to ^{125}I-IUdR as 1.0, are also indicated. These data show that ^{125}I-ITdU and ^{125}I-ITAU were highly resistant to C–N glycoside cleavage reaction by recombi-

TABLE 3
Cell Uptake by LL/2, L-M, and L-M (TK$^-$) Cell Lines

Nucleoside	Tracer uptake* (relative uptake ratio)		
	LL/2	L-M	L-M (TK$^-$)
IUdR	539.7 ± 81.7 (6.9)	77.8 ± 7.4† (2.8)	27.9 ± 2.9
ITdU	226.7 ± 13.1 (20.8)	10.9 ± 1.5† (2.8)	3.9 ± 0.6
ITAU	1.1 ± 0.0 (0.6)	1.7 ± 0.3‡ (1.4)	1.2 ± 0.2

*Tracer uptake = pmol/mg protein/h.
†$P < 0.0005$ compared with L-M (TK$^-$).
‡$P < 0.05$ compared with L-M (TK$^-$) (Student *t* test).
Data in parentheses in LL/2 row and L-M row indicate relative uptake ratios of LL/2 compared with those of L-M cells and relative uptake ratios of L-M compared with those of L-M (TK$^-$), respectively.

SOCIETY OF NUCLEAR MEDICINE

TABLE 4
Biodistribution of ^{125}I-IUdR in Normal Mice (n = 3)

Organ	1 h	1.5 h	2 h	8 h	18 h
Blood	7.6 ± 0.8	5.4 ± 1.2	5.3 ± 0.5	1.1 ± 0.1	0.8 ± 1.1
Spleen	4.7 ± 0.6	4.6 ± 1.2	4.7 ± 2.2	3.1 ± 1.5	1.7 ± 0.9
Intestine	5.0 ± 0.2	3.3 ± 0.7	4.5 ± 0.5	2.4 ± 0.2	1.4 ± 0.4
Thymus	6.6 ± 1.1	4.4 ± 1.6	4.3 ± 1.0	1.8 ± 0.3	1.8 ± 1.5
Femur	4.5 ± 0.5	3.6 ± 0.8	3.7 ± 0.5	1.6 ± 0.1	1.1 ± 0.4
Thyroid	113.0 ± 30.8	80.7 ± 51.9	112.1 ± 22.3	32.9 ± 13.5	9.7 ± 8.0
Lung	5.1 ± 0.4	3.6 ± 0.8	3.6 ± 0.3	0.9 ± 0.4	0.6 ± 0.7
Heart	2.8 ± 0.5	2.1 ± 0.5	1.9 ± 0.1	0.4 ± 0.0	0.3 ± 0.3
Muscle	1.4 ± 0.2	1.5 ± 0.3	1.4 ± 0.5	0.3 ± 0.1	0.1 ± 0.2
Liver	2.7 ± 0.4	2.1 ± 0.5	1.9 ± 0.2	0.4 ± 0.1	0.3 ± 0.3
Brain	0.3 ± 0.0	0.2 ± 0.1	0.2 ± 0.0	0.0 ± 0.0	0.0 ± 0.0
Kidney	5.9 ± 0.4	4.8 ± 1.5	3.4 ± 0.3	0.7 ± 0.1	0.6 ± 0.8

Data are expressed as percentage injected dose per gram (mean ± SD).

nant thymidine phosphorylase. The relative IU formation of ^{125}I-ITdU and ^{125}I-ITAU was 0.03 and <0.01, respectively.

Cell Uptake Study with LL/2, L-M, and L-M (TK$^-$) Cell Lines

Table 3 shows the results of the comparative cell uptake studies. The percentage of S-phase cell fraction values of LL/2, L-M, and L-M (TK$^-$) in this experiment were 47%, 32%, and 37%, respectively. A comparison between L-M and L-M (TK$^-$) uptake data showed that ^{125}I-IUdR and ^{125}I-ITdU exhibited significant cytosolic thymidine kinase–dependent uptake (P <0.0005; Student t test). ^{125}I-ITAU showed a significant but slight thymidine kinase–dependent cell uptake ($P < 0.05$; Student t test). The net uptake value of ^{125}I-IUdR is greater than that of ^{125}I-ITdU in the 3 cell lines. The relative uptake ratio of LL/2 compared with that of L-M showed that ^{125}I-ITdU is more drastically incorporated into the highly proliferating cells than is ^{125}I-IUdR.

DNA Incorporation

Figure 2A shows the time course of the net radioactivity incorporation into the tumor cell lines and the net radioactivity accumulation in the subfractions. ^{125}I-ITdU showed a time-dependent linear incorporation into the tumor cell lines tested. Most of the accumulated radioactivity was found in the DNA subfraction. Figure 2B shows the relative percentage distribution of radioactivity in each fraction. Radioactivity was rapidly distributed into the DNA subfraction. The percentage of the DNA subfraction at 60 min was the same as that of thymidine (*9*).

Biodistribution in Normal Mice

To evaluate the in vivo stability of radioiodination and proliferation-selective uptake of ^{125}I-ITdU and ^{125}I-ITAU, we compared the biodistribution of the nucleoside derivatives in normal mice. ^{125}I-ITdU and ^{125}I-ITAU displayed better in vivo radioiodination stability with a lower thyroid uptake than did ^{125}I-IUdR at all experimental time points (Tables 4–6). ^{125}I-ITdU and ^{125}I-ITAU showed a faster blood clearance than ^{125}I-IUdR and a rapid urinary excretion (Tables 4–7). ^{125}I-ITdU displayed a higher and better retention in proliferating organs (thymus, spleen, intestine, and femur) than in nonproliferating organs (brain, muscle, liver,

TABLE 5
Biodistribution of ^{125}I-ITdU in Normal Mice (n = 3)

Organ	1 h	1.5 h	2 h	8 h	18 h
Blood	2.5 ± 0.3	2.6 ± 0.6	1.6 ± 0.7	0.7 ± 0.2	0.1 ± 0.0
Spleen	1.1 ± 0.1	1.7 ± 0.3	1.1 ± 0.3	0.5 ± 0.1	0.3 ± 0.0
Intestine	1.9 ± 0.1	1.9 ± 0.5	1.7 ± 0.4	1.7 ± 0.5	0.9 ± 0.1
Thymus	1.8 ± 0.1	1.8 ± 0.4	1.4 ± 0.7	2.2 ± 1.3	1.1 ± 0.4
Femur	1.0 ± 0.1	1.0 ± 0.2	0.9 ± 0.2	0.7 ± 0.1	0.2 ± 0.0
Thyroid	23.0 ± 6.4	23.1 ± 12.5	16.3 ± 9.7	16.0 ± 2.7	1.1 ± 0.3
Lung	1.4 ± 0.1	1.5 ± 0.3	1.1 ± 0.5	0.5 ± 0.1	0.1 ± 0.0
Heart	1.0 ± 0.1	1.3 ± 0.3	0.8 ± 0.4	0.2 ± 0.1	0.0 ± 0.0
Muscle	0.5 ± 0.2	0.7 ± 0.2	0.5 ± 0.2	0.1 ± 0.1	0.0 ± 0.0
Liver	1.1 ± 0.2	1.5 ± 0.4	0.9 ± 0.5	0.2 ± 0.1	0.0 ± 0.0
Brain	0.1 ± 0.0	0.2 ± 0.1	0.1 ± 0.0	0.0 ± 0.0	0.0 ± 0.0
Kidney	9.5 ± 3.5	5.8 ± 4.1	1.9 ± 1.7	0.5 ± 0.1	0.1 ± 0.0

Data are expressed as percentage injected dose per gram (mean ± SD).

SOCIETY OF NUCLEAR MEDICINE

TABLE 6
Biodistribution of ^{125}I-ITAU in Normal Mice ($n = 3$)

Organ	1 h	1.5 h	2 h	8 h	18 h
Blood	3.7 ± 0.4	4.5 ± 0.3	3.7 ± 0.8	0.4 ± 0.1	0.1 ± 0.1
Spleen	1.6 ± 0.1	2.3 ± 0.4	2.1 ± 0.5	0.2 ± 0.1	0.1 ± 0.0
Intestine	1.8 ± 0.2	2.4 ± 0.4	2.1 ± 0.6	0.4 ± 0.1	0.1 ± 0.1
Thymus	2.1 ± 0.5	3.0 ± 1.0	2.3 ± 0.6	0.2 ± 0.2	0.1 ± 0.0
Femur	1.4 ± 0.1	1.6 ± 0.1	1.4 ± 0.3	0.2 ± 0.1	0.1 ± 0.0
Thyroid	46.1 ± 5.2	57.2 ± 10.5	60.3 ± 27.6	18.6 ± 13.0	4.1 ± 2.2
Lung	2.3 ± 0.2	2.7 ± 0.3	2.4 ± 0.6	0.3 ± 0.1	0.1 ± 0.1
Heart	1.5 ± 0.3	2.1 ± 0.1	1.6 ± 0.3	0.2 ± 0.0	0.0 ± 0.0
Muscle	0.9 ± 0.1	1.3 ± 0.1	1.0 ± 0.2	0.1 ± 0.0	0.0 ± 0.0
Liver	1.4 ± 0.2	2.0 ± 0.2	1.4 ± 0.4	0.1 ± 0.0	0.0 ± 0.0
Brain	0.4 ± 0.0	0.5 ± 0.1	0.3 ± 0.1	0.0 ± 0.0	0.0 ± 0.0
Kidney	7.2 ± 2.3	5.0 ± 0.3	3.6 ± 0.6	0.3 ± 0.1	0.1 ± 0.1

Data are expressed as percentage injected dose per gram (mean ± SD).

and lung), as did ^{125}I-IUdR at 18 h after injection (Tables 4 and 5 and Fig. 3). As a result, ITdU displayed a statistically significant target (proliferating organs) for its background (blood) ratio compared with IUdR in the thymus and intestine ($P < 0.05$; Student t test; Fig. 2). The ^{125}I-ITAU did not show any preferential proliferation in organ uptake (Table 6), as would be expected according to the in vitro study.

DISCUSSION

In this study we successfully determined the rationale and performed the synthesis and fundamental evaluations of radioiodinated ITdU and ITAU. In particular, the higher in vivo radioiodination stability and rapid DNA-incorporating nature of ITdU caused a selective and preferential uptake in the proliferating organs.

The radiolabeling of ITdU and ITAU used iodine as the oxidant for the destannylation reaction. This reaction is not suitable for obtaining high specific activity for practical imaging. However, in this screening study, the specific activity was sufficient for the evaluation. In addition, both ITdU and ITAU contain sulfide, which may be oxidized by the strong oxidant and might result in sulfoxide. To avoid this reaction, we have selected mild oxidative conditions. Nevertheless, in in vivo experiments, the lower specific activity would lead us to underestimate the potential of these compounds. In an earlier study, 5-^{82}Br-bromo-1-(2-fluoro-2-deoxy-β-D-ribofuranosyl)uracil showed the absence of tumor selectivity and low uptake in the tumor (*6*). The authors concluded that this compound is not suitable as an imaging agent. In contrast, very recently, the same structured compound 5-^{76}Br-bromo-2′-fluoro-2′-deoxyuridine was proven to be a potentially good tracer for the assessment of tumor proliferation (*17–18*). In this case, the specific activity of the compound was significantly higher than that in the previous study. The specific activity of the more recent study (150 GBq/μmol) was 3–4 × 10^3 times higher than that in the previous study (40–50 GBq/mmol). Moreover, in the previous study, 150–400 nmol of compound was injected per mouse, whereas in the recent study mice received <0.02 nmol of compound per mouse. It has been estimated that the hypothetic endogenous pool of thymidine in mice was 50 nmol per mouse (*19*), and the in vivo tracer uptake of radiolabeled nucleosides may be affected by those specific activities. Thus, the establishment of a suitable labeling method for the destannylation reaction of ITdU with the goal of obtaining a compound with high specific activity will be in great demand.

The nucleoside kinases assay clarified that ITdU, with a substitution of the furanose ring oxygen by sulfur, did not highly interfere with nucleoside kinase phosphorylation activity. Moreover, ITdU exhibited cytosolic thymidine kinase–dependent uptake in L-M cells. On the other hand,

TABLE 7
Urinary Excretion of Iodonucleosides in Normal Mice ($n = 3$)

Nucleoside	1 h	1.5 h	2 h	8 h	18 h
IUdR	18.6 ± 6.7	21.6 ± 6.6	23.4 ± 4.5	48.4 ± 5.7	54.7 ± 9.1
ITdU	57.5 ± 4.7	53.6 ± 6.1	56.5 ± 7.7	73.1 ± 6.1	71.4 ± 14.6
ITAU	50.2 ± 5.4	40.0 ± 7.6	43.2 ± 6.8	70.6 ± 3.3	64.8 ± 5.5

Data are expressed as percentage injected dose (mean ± SD).

ITAU did not show remarkable phosphorylation activity or notable thymidine kinase–dependent cell uptake. This is understandable because ITAU has 2′-up stereochemistry (arabino configuration), which is important for the recognition of virus-encoded thymidine kinase but not for the recognition of host kinase (*13*). These results suggested that ITdU was phosphorylated by the cytosolic thymidine kinase and might be retained in the cells in a kinase-dependent manner, although we have never characterized the responsible nucleoside kinase. In addition, an in vitro cell metabolism study of ITdU clarified that ITdU was effectively and specifically incorporated into a DNA fraction. Therefore, ITdU is readily phosphorylated and used as a substrate for DNA synthesis. This DNA-incorporating nature of ITdU might be useful as a proliferation marker after therapeutic intervention. A discrepancy has been reported between DNA incorporation of thymidine and the thymidine uptake in the cytoplasm, which is not incorporated into the DNA (*20–22*). The long physical half-lives of iodine radioisotopes ^{124}I (4.2 d), ^{131}I (8.1 d), and ^{123}I (13 h) are suitable for waiting for the washout of non-DNA–incorporated radioactivity.

As expected in the rationale we developed, ITdU and ITAU were highly resistant to C–N glycoside cleavage reaction by recombinant thymidine phosphorylase. The exact mechanism of this stabilization effect of sulfur substitution is still unclear. The hypothetic mechanism of pyrimidine phosphorolysis is the S_{N1}-type reaction—that is, the polarization of the N1–C1′ glycosidic bond of nucleoside (*23*). This partial positive charge at C1′ could be stabilized by the formation of an oxocarbenium ion at O4′. Accordingly, the higher stability of the 4′-thio analogs may derive from the lower stability of the cyclic thiocarbenium ion compared with the corresponding oxocarbenium ion.

It have been suggested that there are 2 mechanisms of deiodination of 5-halogen (*24–26*). One is the thymidine phosphorylase–dependent deiodination, and the other is the 5-halogen substitution reaction of monophosphorylated nucleoside by the thymidylate synthase. It is well known that IUdR is rapidly catabolized by phosphorylytic cleavage to iodouracil and deoxyribose by the ubiquitous enzyme pyrimidine phosphorylase (*25*). Iodine is rapidly lost nonenzymatically from iodouracil after its enzymatic reduction by the uracil reductase to 5-iodo-5,6-dihydrouracil (*25*,*26*). Therefore, we hypothesized that stabilizing the C–N glycosidic bond by furanose ring oxygen-to-sulfur substitution would induce high stability in the 5-halogen bond. In line with this hypothesis, ITdU and ITAU displayed better in vivo radioiodination stability with a lower thyroid uptake than did IUdR at all of the experimental time points. However, some deiodination still occurred. The thymidylate synthase and also direct reductive deiodination of 5-iodine might cause this deiodination.

The in vivo biodistribution study of ITdU in normal mice showed that ITdU has a better retention in the proliferating organs (thymus, spleen, intestine, and femur) than in non-proliferating organs (brain, muscle, liver, and lung) at 18 h after injection. The proliferation organ-to-blood ratio of ITdU was variable in the different proliferation organs. However, IUdR tended to have the same proliferation organ-to-blood ratios in the various proliferation organs. Preliminarily, we calculated the percentage of the S-phase cell fraction of thymus and spleen of normal mice to be 10% and 4%, respectively, by cytometric analysis (data not shown). Therefore, the variable proliferation organ-to-blood ratio of ITdU might reflect the difference of the cell proliferation activity in each organ.

However, the specific and significant uptake to the proliferating organ needs a greater washout and clearance of exchangeable fraction of background activity. The metabolite and relatively lower specific activity of ITdU would affect the specific imaging in the early time course. Therefore, extensive validation studies of ITdU will be needed to know whether it is a practical proliferation-imaging agent.

CONCLUSION

We applied the new strategy of stabilizing the glycosidic bonds of nucleosides without interfering with their affinity to the cytosolic nucleoside kinases by substituting 4′-sulfur for 4′-oxygen. Using this strategy, ITdU exhibited a high resistance to the glycosidic bond cleavage reaction provoked by thymidine phosphorylase, while keeping an affinity to nucleoside kinases. The higher in vivo radioiodination stability and rapid DNA incorporation of ITdU compared with IUdR brought about a preferential uptake of radioactivity in the proliferating organs. These facts suggest that radioiodinated ITdU is potentially useful as a proliferation-imaging agent and that further studies should clarify the usefulness of this compound as a tumor-imaging agent.

REFERENCES

1. Blasberg RG, Roelcke U, Weinreich R, et al. Imaging brain tumor proliferative activity with [^{124}I]iododeoxyuridine. *Cancer Res.* 2000;60:624–635.
2. Tjuvajev JG, Macapinlac HA, Daghighian F, et al. Imaging of the brain tumor proliferative activity with [^{131}I]iododeoxyuridine. *J Nucl Med.* 1994;35:1407–1417.
3. Choi SR, Chumpradit S, Kung MP, Kung HF. Novel iodinated nucleoside as a potential tumor imaging agent [abstract]. *J Nucl Med.* 2000;41(suppl):233P.
4. Gati WP, Misra HK, Knaus EE, Wiebe LI. Structural modifications at the 2′- and 3′-positions of some pyrimidine nucleosides as determinants of their interaction with the mouse erythrocyte nucleoside transporter. *Biochem Pharmacol.* 1984; 33:3325–3331.
5. Eriksson S, Kierdaszuk B, Munch-Peterson B, Oberg B, Johansson NG. Comparison of the substrate specificities of human thymidine kinase 1 and 2 and deoxycytidine kinase toward antiviral and cytostatic nucleoside analogs. *Biochem Biophys Res Commun.* 1991;176:586–592.
6. Merecer JR, Xu Li-H, Knaus EE, Wiebe LI. Synthesis and tumor uptake of 5-^{82}Br- and 5-^{131}I-labeled 5-halo-1-(2-fluoro-2-deoxy-β-D-ribofuranosyl)uracils. *J Med Chem.* 1989;32:1289–1294.
7. Tjuvajev JG, Chen SH, Joshi A, et al. Imaging adenoviral mediated herpes virus thymidine kinase gene transfer and expression in vivo. *Cancer Res.* 1999;59: 5186–5193.
8. Wang J, Eriksson S. Phosphorylation of the anti-hepatitis B nucleoside analog 1-(2′-deoxy-2′-fluoro-1-β-D-arabinofuranosyl)-5-iodouracil (FIAU) by human cytosolic and mitochondrial thymidine kinase and implications for cytotoxicity. *Antimicrob Agents Chemother.* 1996;40:1555–1557.
9. Toyohara J, Azuma-Kato M, Waki A, et al. Basis of FLT as a cell proliferation marker: comparative uptake studies with thymidine, arabinothymidine and FDG,

and cell-analysis in 22 asynchronously growing tumor cell lines [abstract]. *J Nucl Med.* 2001;42(suppl):83P.
10. Miura G, Gordon R, Montogomery JA, Chaing P. 4′-Thioadenosine as a novel inhibitor of S-adenosylhomocysteine hydrolase and an inducer for the differentiation of HL-60 human leukemia cell. In: Nyhan E, Thompson L, Watts R, eds. *Purine Pyrimidine Metabolism in Man: V.* New York, NY: Plenum Press; 1986:667–672.
11. Parks RE Jr, Stoecker JD, Cambor C, Savarese TM, Crabtree GW, Chu S-H. Purine nucleoside phosphorylase and 5′-methylthioadenosine phosphorylase: targets of chemotherapy. In: Sartorelli AC, Lazo JS, Bertino JR, eds. *Molecular Actions and Targets for Cancer Chemotherapeutic Agents.* New York, NY: Academic Press; 1981:229–252.
12. Rahim SG, Trivedi N, Bogunovic-Batchelor MV, et al. Synthesis and anti-herpes virus activity of 2′-deoxy-4′-thiopyrimidine nucleosides. *J Med Chem.* 1996;39: 789–795.
13. Yoshimura Y, Watanabe M, Satoh H, et al. A facile, alternative synthesis of 4′-thioarabinonucleosides and their biological activities. *J Med Chem.* 1997;40: 2177–2183.
14. Wolcott RM, Colacino JM. Detection of thymidine kinase activity using an assay based on the precipitation of nucleoside monophosphates with lanthanum chloride. *Anal Biochem.* 1989;178:38–40.
15. Nottebrock H, Then R. Thymidine concentrations in serum and urine of different animal species and man. *Biochem Pharmacol.* 1977;26:2175–2179.
16. Quackanbush RC, Shields AF. Local re-utilization of thymidine in normal mouse tissues as measured with iododeoxyuridine. *Cell Tissue Kinet.* 1988;21:381–387.
17. Lu L, Bergström M, Fasth K-J, Långström B. Synthesis of [^{76}Br]bromofluorodeoxyuridine and its validation with regard to uptake, DNA incorporation, and excretion modulation in rats. *J Nucl Med.* 2000;41:1746–1752.
18. Borbath I, Grégorie V, Bergström M, Laryea D, Långstrom B, Pauwels S. Use of 5-[^{76}Br]-2′-fluoro-2′-deoxyuridine as a ligand for tumor proliferation: validation in an animal model. *Eur J Nucl Med.* 2002;29:19–27.
19. Lee D-J, Prensky W, Krause G, Hughes WL. Blood thymidine level and iododeoxyuridine incorporation and reutilization in DNA in mice given long acting thymidine pellets. *Cancer Res.* 1976;36:4577–4583.
20. Haberkorn U, Bellemann ME, Altmann A, et al. F-18-Fluoro-2-deoxyglucose uptake in rat prostate adenocarcinoma during chemotherapy with 2′,2′-difluoro-2′-deoxycytidine. *J Nucl Med.* 1997;38:1215–1221.
21. Haberkorn U, Bellemann ME, Brix G, et al. Apoptosis and changes in glucose metabolism after treatment of Morris hepatoma with gemcitabine. *Eur J Nucl Med.* 2001;28:418–425.
22. Haberkorn U, Altmann A, Kamencic H, et al. Glucose transport and apoptosis after gene therapy with HSV thymidine kinase. *Eur J Nucl Med.* 2001;28:1690–1696.
23. Pugmire MJ, Ealick SE. The crystal structure of pyrimidine nucleoside phosphorylase in a closed conformation. *Structure.* 1998;6:1467–1479.
24. Garrett C, Wataya Y, Santi DV. Thymidylate synthase: catalysis of degradation of 5-bromo- and 5-iodo-2′-deoxyuridylate. *Biochemistry.* 1979;18:2798–2804.
25. Prusoff WH, Jaffe JJ, Gunther H. Studies in the mouse of the pharmacology of 5-iododeoxyuridine, an analog of thymidine. *Biochem Pharmacol.* 1960;3:110–121.
26. Kim BD, Keene S, Bodnar JK, Sander EG. Role of enzymatically catalyzed 5-iodo-5,6-dihydrouracil ring hydrolysis on the dehalogenation of 5-iodouracil. *J Biol Chem.* 1976;251:6909–6914.

SOCIETY OF NUCLEAR MEDICINE